Food and Chemical Toxicology 137 (2020) 111127

Contents lists available at ScienceDirect

Food and Chemical Toxicology

journal homepage: www.elsevier.com/locate/foodchemtox

A physiologically based pharmacokinetic model of doxycycline for predicting tissue residues and withdrawal intervals in grass carp (*Ctenopharyngodon idella*)

Ning Xu[a,b], Miao Li[a], Wei-Chun Chou[a], Zhoumeng Lin[a,*]

[a] Institute of Computational Comparative Medicine (ICCM), Department of Anatomy and Physiology, College of Veterinary Medicine, Kansas State University, Manhattan, KS, 66506, USA

[b] Yangtze River Fisheries Research Institute, Chinese Academy of Fishery Sciences, Wuhan, 430223, China

ARTICLE INFO

Keywords:
Doxycycline
Physiologically based pharmacokinetic (PBPK) model
Grass carp
Drug residue
Withdrawal time
Food safety

ABSTRACT

The extensive use of doxycycline in aquaculture results in drug residue violations that negatively impact human food safety. This study aimed to develop a physiologically based pharmacokinetic (PBPK) model for doxycycline to predict drug residues and withdrawal times (WTs) in grass carp (*Ctenopharyngodon idella*) after daily oral administration for 3 days. Physiological parameters including cardiac output and organ weights were measured experimentally. Chemical-specific parameters were obtained from the literature or estimated by fitting to the observed data. The model properly captured the observed kinetic profiles of doxycycline in tissues (i.e., liver, kidney, muscle + skin and gill). The predicted WT in muscle + skin by Monte Carlo analysis based on sensitive parameters identified at 24 h after drug administration was 41 d, which was similar to 43 d calculated using the tolerance limit method. Sensitivity analysis identified two additional sensitive parameters at 6 weeks: intestinal transit rate constant and urinary elimination rate constant. The predicted WT in muscle + skin based on sensitive parameters identified at 6 weeks was 54 d. This model provides a useful tool to estimate tissue residues and withdrawal times for doxycycline in grass carp and also serves a foundation for extrapolation to other fish species and other tetracyclines.

1. Introduction

Antibiotics are commonly used in aquaculture in many countries (Liu et al., 2017; Lulijwa et al., 2019). Drugs residues in fish-derived food products can enter into the human body through food chain. Excessive exposure to drug residues at a concentration higher than maximum residue limit (MRL) or tolerance can cause various adverse reactions in humans, such as allergies, vomiting, diarrhea and hormone-like reactions (Baynes et al., 2016). To ensure fish-derived food safety for humans, it is important to establish a novel method to rapidly and accurately provide drug residue and withdrawal time information in fish products.

The traditional approach for monitoring drug residue in edible tissues of fish and other food-producing animals relies on animal experiments and analytical equipment, which is time-consuming, labor-intensive and requires a number of animals especially when determining the metabolic profile, potential toxicity and withdrawal time (WT) (Huang et al., 2015b). Currently, there are several hundred of aquatic species cultured all over the world, including 369 finfishes (involving 5 hybrids), 109 molluscs, 64 crustaceans, 7 amphibian and reptiles (excluding alligators, caimans or crocodiles), 9 aquatic invertebrates and 40 aquatic algae (FAO, 2018). Also, more than 50 therapeutic drugs are approved to use in aquaculture, including antiparasitics, antibiotics, disinfectants, and antifungals (Liu et al., 2017; Lulijwa et al., 2019). It will be an enormous project if the tissue residue depletion kinetics and withdrawal time information are determined for all drugs in every species experimentally. Hence, a quantitative tool that can be used to predict drug residue depletion kinetic profiles and withdrawal times, and can be extrapolated across animal species, exposure scenarios, and to other structurally similar drugs is urgently needed. In this regard, physiologically based pharmacokinetic (PBPK) models are an ideal tool that can address this scientific need as it is a mechanism-based computational approach combining species-specific physiological parameters, chemical-specific dynamic information and other relevant

* Corresponding author. Institute of Computational Comparative Medicine (ICCM), Department of Anatomy and Physiology, College of Veterinary Medicine, Kansas State University, 1800 Denison Avenue, P200 Mosier Hall, Manhattan, KS, 66506, USA.

E-mail addresses: xuning@yfi.ac.cn (N. Xu), miaoli@ksu.edu (M. Li), weichunc@vet.k-state.edu (W.-C. Chou), zhoumeng@ksu.edu (Z. Lin).

https://doi.org/10.1016/j.fct.2020.111127
Received 8 October 2019; Received in revised form 14 December 2019; Accepted 9 January 2020
Available online 13 January 2020
0278-6915/

Abbreviations

AUC	area under concentration–time curve
$AUC_{0-\infty}$	area under concentration–time curve from 0 to ∞
C_{max}	peak concentration
CV	coefficient of variance
DC	doxycycline
EMA	European Medicines Agency
Ka	absorption rate constant of foregut and midgut
Kah	absorption rate constant of hindgut
KbileC	biliary elimination rate constant
KehcC	rate constant for enterohepatic circulation
Kfeces	fecal elimination rate constant
Kint	intestinal transit rate constant
KurineC	urinary elimination rate constant
MAPE	mean absolute percentage error
MC	Monte Carlo
MS222	tricaine methanesulfonate
MRL	maximum residue limit
NSC	normalized sensitivity coefficient
PB	plasma protein binding percentage
PBPK	physiologically based pharmacokinetic
PC	tissue/plasma partition coefficient
PK	pharmacokinetics
R^2	determination coefficient
SA	sensitivity analysis
$t_{1/2\alpha}$	distribution half-life
$t_{1/2\beta}$	elimination half-life
Vss	volume of distribution at steady-state
WHO	World Health Organization
WT	withdrawal time.

important influential factors to simulate the absorption, distribution, metabolism and excretion of chemicals in an organism using mathematical equations (Lin et al., 2016a).

Many PBPK models have been developed to predict drug residues and WTs in food animals, such as cattle, swine, and chickens (Buur et al., 2006; Leavens et al., 2014; Yang et al., 2015, 2019; Li et al., 2017; Zeng et al., 2017, 2019). As for fish, there are many PBPK models for environmental health risk assessment (Grech et al., 2017, 2019), but only a few models for food safety assessment. Law (1999) and colleagues reported a PBPK model of oxytetracycline in cultured chinook salmon (*Oncorhynchus tshawytscha*) in late 1990s. However, due to some limitations in computational technology and lack of complete guidance documents for drug residue and WT predictions at that time, there was no new published PBPK models for drugs in fish for the purpose of predicting tissue residues and WTs in the subsequent 10 years. Recently, a PBPK model of florfenicol in crucian carp (*Carassius auratus*) was established to predict florfenicol's pharmacokinetic profile in various tissues after a single oral or intramuscular administration, but the model cannot be used to predict WTs because the population variability was not considered in the model (Yang et al., 2013). Therefore, to meet modern demand of drug residue surveillance, a PBPK model that can predict drug residue and WTs in fish needs to be developed.

Doxycycline (DC) is one of the most widely used antibiotics of tetracyclines in aquaculture with broad-spectrum and efficient activity against *Aeromonas hydrophila*, *Fibrobacter columnaris*, *Pseudomonas fluorescens*, and *Vibrio vulnificus* (Shireman et al., 1976; Liu et al., 2019). The label use of DC is at the dosage of 20 mg/kg/day for 3–5 days in China. The MRLs in fish (muscle + skin) are 100 (EU, 2015), 100 (MAA, 2017), and 50 μg/kg (JFCRF, 2006) in Europe, China and Japan, respectively. Residue violations of DC in fish products are reported partly due to lack of fast and effective surveillance tools. In our recent studies, we collected extensive pharmacokinetic and tissue residue depletion data of DC in grass carp (*Ctenopharyngodon idella*) following single and repeated daily oral administrations (Xu et al., 2019a, 2019b). These new data make it feasible to develop a reliable PBPK model in grass carp. Grass carp is a predominately cultured fish species in global aquaculture with the prime production of more than 6.07 million tons per year (FAO, 2018), thus it is important to establish a PBPK model in this species. The objective of this study was to develop a PBPK model coupled with Monte Carlo (MC) analysis for predicting tissue residues and WTs of DC after multiple oral administrations in grass carp. The PBPK model will provide a foundation to predict aquatic drug residues and WTs in fish to help food safety assessment.

2. Materials and methods

2.1. Chemicals and reagents

Analytical standards of Evans blue (95%) and DC (98%) were purchased from Dr. Ehrenstorfer GmbH. (Augsburg, Germany). The DC powder (98%) used for intravenous administration was provided by Zhongbo Aquaculture Biotechnology Co. Ltd. (Wuhan, China). The anesthetic tricaine methanesulfonate (MS222) was purchased from Aibo Biotechnology Co. Ltd. (Wuhan, China). The 22 G needles, 23 G needles, PE-40 and PE-20 polyethylene tubes, 1 mL syringes, surgical scissors, surgical needles, scalpels, tweezers, surgical suture, heparin and 0.9% saline were obtained from Provence Biotechnology Co. Ltd. (Wuhan, China). The 1.5 mL vials and centrifugal tubes were purchased from Shanghai CNW Technologies (Shanghai, China).

2.2. Animals

The culture facility of Yangtze River Fisheries Research Institute (Wuhan, China) provided experimental grass carp (400.5 ± 20.3 g, 12 months of age, mixed genders). The fish were held in tanks (10 fish each tank; volume of each tank: 480 L) and acclimated for 14 days fed with drug-free feed that was composed of 28.00% crude proteins, 7.06% crude fat, 15.00% crude fiber, 8.75% moisture, and 15.63% ash made by the Nutritional Research Group in Yangtze River Fisheries Research Institute, Chinese Academy of Fishery Sciences, Wuhan, China. The relevant water quality parameters were monitored daily and maintained in appropriate ranges, including nitrite nitrogen concentrations (< 0.072 mg/L), total ammonia nitrogen concentrations (< 0.74 mg/L), dissolved oxygen concentrations (6.1–7.0 mg/L), and pH values (7.2 ± 0.2). The water temperature was controlled by aquarium heater and air-conditioner and maintained at 24 ± 0.5 °C. Bubbling air with air-stones was used to hold oxygen in water to achieve saturated status. All protocols involving animals were approved by the Fish Ethics Committee of Yangtze River Fisheries Research Institute, Chinese Academy of Fishery Sciences, Wuhan, China.

2.3. Determination of cardiac output

The procedure to measure cardiac output using indicator dilution method was based on Barron et al. (1987) with some modifications. In brief, a custom 22 G, 5 cm needle was connected to 20 cm of PE-40 to serve as the dorsal aorta cannula. The other end of the cannula was attached to a 1 mL syringe filled with 0.5% heparinized solution. The fish was weighed and anaesthetized with 50 mg/L MS222 solution and the tip of the snout was medially pierced with surgical scissors. A 22 G needle was inserted into the dorsal aorta and a proper amount of 0.5%

heparinized solution was injected to prevent blood reflux and coagulation in the tube. The other end of the cannula was passed through the hole made by surgical scissors to be utilized to collect blood samples, and then fixed with sutures.

The heart cannula included a 4 cm, 22 G needle with a 90° bend at the end connected to 50 cm of PE-20. The cannula was also filled with 0.5% heparinized solution. Then the needle was inserted medially between the pectoral fins avoiding the bones, and an appropriate amount of 0.5% heparinized solution was injected to prevent blood reflux and coagulation in the tube. Finally, the heart cannula was fixed with 2–3 abdominal sutures. The preparation of the dorsal aorta or heart should be completed within 10 min as soon as possible. The fish was allowed to recover for about 1 h in a custom tank with 40 L water maintained at the acclimation temperature.

Before initiation of the experiment, blank blood samples were collected from the dorsal aorta cannula. The Evans blue standard was dissolved using 0.9% saline to get a final concentration at 20 mg/mL. Two hundred μL of Evans blue solution (containing 1 mg Evans blue) was withdrawn by 1 mL syringe and injected into the heart from the heart cannula. Blood was collected from dorsal aorta every 5 s. The sample determination and data calculation were described in the Supplementary Materials.

2.4. Measurements of organ weights

The fish (n = 10) was weighed and anaesthetized with 50 mg/L MS222 solution. The blood was collected from caudal vessels and dorsal aorta as much as possible. The gills were collected using surgical scissors. The scales were removed by surgical scissors, and then all skin was collected by surgical scissors and scalpels. Subsequently, fish abdomen was opened to collect liver, kidney, intestine, bile, spleen, swim bladder and heart. Afterwards, the muscle was removed from the bone. Scales and corpse were attributable to remainder. All collected organs were weighed.

2.5. Intravenous pharmacokinetic study

The DC power was dissolved in 0.9% saline to get a final concentration of 20 mg/mL and a proper amount of hydrochloric acid was added to make DC completely soluble, which was used for intravenous administration. Prior to injection of DC, fish were anaesthetized with MS222 (50 mg/L) and weighted. The first step was to confirm the position of the needle in the caudal vein by aspirating blood into the syringe, and then inject the corresponding volume of DC solution at dose of 20 mg/kg. If the fish was heavily bleeding after withdrawal of the needle or the needle had translocated during injection, the fish was excluded from the study and replaced. After intravenous administration, approximately 2 mL of blood was taken from the caudal vein away from the injection site from six fish at each sampling time point of 0.08, 0.17, 0.5, 1, 2, 4, 6, 8, 16, 24, 48, 72, 96, and 120 h. Blood samples were centrifuged at 1500 *g* for 5 min. The plasma was collected and stored at −20 °C until analysis. The sample preparation and determination were based on our published protocol (Xu et al., 2019b). Phoenix WinNonlin 8.0 (Certara, Inc., Princeton, NJ, USA) was used to calculate the pharmacokinetic (PK) parameters of obtained data.

2.6. Model structure

In the present study, a seven-compartment PBPK model was structured, including plasma, liver, kidney, muscle + skin, gill, richly perfused tissues, and slowly perfused tissues. The model structure is shown in Fig. 1. All compartments were assumed as to be well-stirred and perfusion-limited. Since European Medicines Agency (EMA) has designated the muscle + skin together as the edible tissue in fish (EMA, 2009). For the perspective of food safety assessment, the muscle + skin was included as an individual compartment. The liver as the main metabolism organ and kidney as the main excretion organ were also modeled as individual compartments. The gill is an important target organ for antibiotics as it is susceptible to pathogens and parasites, hence, it was included as an individual compartment. The rest of body was divided into the richly perfused tissues (e.g., gut, heart, and spleen) and the slowly perfused tissues (e.g., bone and fat). All compartments were defined by a tissue weight and tissue blood flow rate connected with blood circulation system. Since the present study determined drug residue depletion for more than 1 month, body weight changes of the grass carp were considered in the PBPK model. The growth curve equation based on experimental data from common carp (Viola et al., 1983) was incorporated into the present grass carp model because grass carp-specific data were not available and it was shown that grass carp and common carp could reach similar body weights during the same feeding time (Hu et al., 2019). In addition, the absorption system of grass carp is different from other species, hence oral absorption was described in accord with its properties using the equations in Supplementary Materials. Berkeley Madonna (Version 8.3.23.0; University of California at Berkeley, CA, USA) was used to develop the model and run all simulations. Key model equations are explained below. The entire model code is provided and annotated in the Supplementary Materials.

2.7. Model parameterization and calibration

Physiological parameters including cardiac output, body weight, and organ weight fractions (i.e., percentage of each organ to total body weight) were experimentally measured as described above. Blood flows

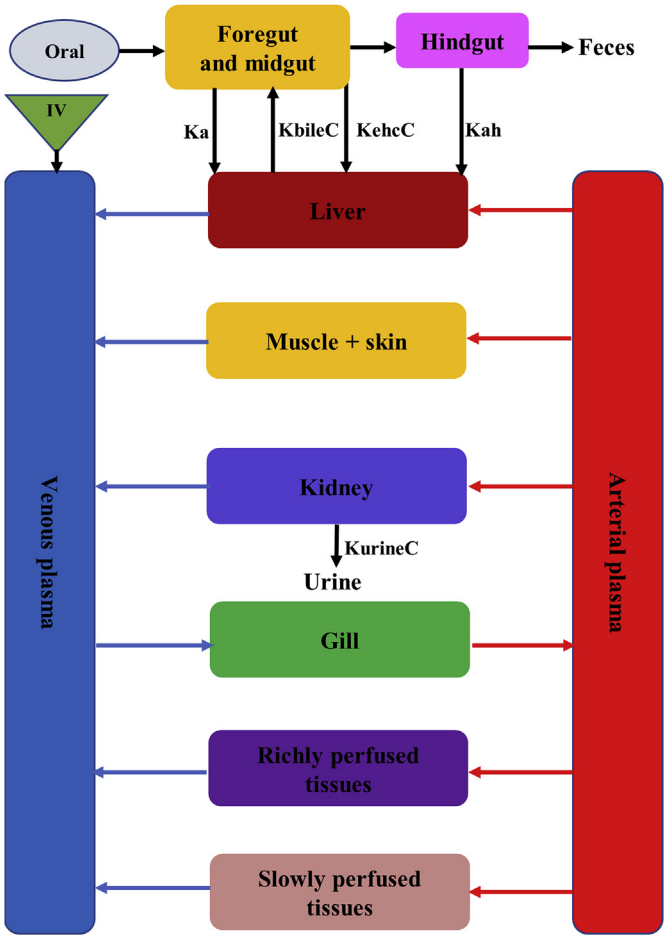

Fig. 1. A schematic diagram of a physiologically based pharmacokinetic (PBPK) model for doxycycline in grass carp (*Ctenopharyngodon idella*). Descriptions of parameters are provided in Table 1. Model code in MMD file is provided in the Supplementary Material.

were based on the values in rainbow trout (*Salmo gairdneri Richardson*) due to lack of grass carp-specific experimental data (Barron et al., 1987; Law et al., 1991). The ratio of arterial blood to venous blood was based on the value in rodents (Lin et al., 2016b) as fish-specific value is not available. The reported hematocrit of blood in grass carp was used in this model (Yavuzcan-Yıldız and Kırkavgaç-Uzbilek, 2001).

As for chemical-specific parameters, partition coefficients (PCs) in various tissues were calculated using the AUC method based on the experimental pharmacokinetic data in grass carp after a single oral dose (Xu et al., 2019b). These calculated PC values were further optimized by fitting to the observed tissue residue data (Xu et al., 2019a) using the Curve Fitting module based on the least squares method in Berkeley Madonna (Macey et al., 2009). PCs of richly and slowly perfusion tissues were set the same values as liver and muscle + skin, respectively. The equations used to calculate PCs were presented in the Supplementary Materials. All datasets used for calculating parameters and model calibration are listed in Table S1. The urine elimination rate constant (KurineC) was first estimated by fitting to the plasma dataset following intravenous dosing in grass carp at 20 mg/kg (described above and listed in Table S1). The protein binding ratio (PB) of DC was based on measured data in humans (Pal et al., 2018) due to lack of fish-specific data. The absorption rate constant of foregut and midgut (Ka), absorption rate constant of hindgut (Kah), intestinal transit rate constant (Kint), rate constant for enterohepatic circulation (KehcC), biliary elimination rate constant (KbileC) and fecal elimination rate constant (Kfeces) of DC were not available in grass carp. Consequently, the initial value of Ka was referred to that in swine (Zeng et al., 2017), and the value Kah was set as same value of Ka. The initial values of Kint, KehcC, KbileC and Kfeces were based on those in swine (Li et al., 2019). These initial parameter values were calibrated by the Curve Fitting module in Berkeley Madonna and further optimized with observed residue data (Xu et al., 2019a) by visual inspection if needed. All final parameters are shown in Table 1.

2.8. Evaluation and sensitivity analysis (SA)

Unused external datasets not used in the model calibration were not available for independent model evaluation. Nevertheless, the present model simulation performance was evaluated qualitatively and quantitatively using well-accepted approaches. First, based on World Health Organization (WHO) guidelines, if the simulations matched the measured kinetic profiles and were generally within a factor of two of the measured values, the model was considered reasonable and acceptable (WHO, 2010). The goodness-of-fit of the model was assessed by visual inspection, model convergence and linear regression between simulated and predicted concentrations in plasma and tissues. The determination coefficient (R^2) values were calculated and the model simulation was considered acceptable if R^2 value was equal to or higher than 0.75 (Li et al., 2018). The goodness of fit was also assessed through the mean absolute percentage error (MAPE) value. A simulation with the MAPE value less than 50% was considered as an acceptable prediction (Lin et al., 2017).

Sensitive analysis (SA) was performed by examining influence on 24-h AUC or 1008-h AUC of plasma, liver, kidney, muscle + skin and

Table 1
Physiological parameters and chemical-specific parameters in the PBPK model.

Parameter	Abbreviation	Mean	References
Body weight (kg)	BW	0.450	Experimentally measured
Cardiac output (L/h/kg)	QCC	3.738	Experimentally measured
Tissue volume (fraction of body weight, unitless)			
Blood	Vblood	0.074	Experimentally measured
Arterial blood	VartC	0.015	Lin et al. (2016b)
Venous blood	VvenC	0.059	Lin et al. (2016b)
Liver	VLC	0.004	Experimentally measured
Kidney	VKC	0.004	Experimentally measured
Muscle + skin	VMC	0.386	Experimentally measured
Gill	VGC	0.037	Experimentally measured
Richly perfused tissues	VRC	0.030	Experimentally measured
Slowly perfused tissues	VSC	0.465	Experimentally measured
Blood flow (fraction of cardiac output, unitless)			
Liver	QLC	0.181	Barron et al. (1987); Law et al. (1991)
Kidney	QKC	0.102	Barron et al. (1987); Law et al. (1991)
Muscle	QMC	0.398	Barron et al. (1987); Law et al. (1991)
Richly perfused tissues	QRC	0.010	Barron et al. (1987); Law et al. (1991)
Slowly perfused tissues	QSC	0.309	Barron et al. (1987); Law et al. (1991)
Hematocrit of blood			
	Hematocrit	0.254	Yavuzcan-Yıldız and Kırkavgaç-Uzbilek (2001)
Absorption rate constant (/h)			
	Ka	0.007	Model fitted
	Kah	0.001	Model fitted
Tissue:plasma partition coefficient for the parent drug (unitless)			
Liver	PL	2.821	Calculated/optimized
Kidney	PK	1.064	Calculated/optimized
Muscle	PM	0.901	Calculated/optimized
Gill	PG	2.981	Calculated/optimized
Richly perfused tissues	PR	2.821	Model fitted
Slowly perfused tissues	PS	0.901	Model fitted
Percentage of plasma protein binding (unitless)	PB	0.900	Pal et al. (2018)
Urinary elimination rate constant (L/h/kg)	KurineC	0.019	Model fitted
Intestinal transit rate constant (/h)	Kint	0.0031	Model fitted
Rate constant for enterohepatic circulation (/h/kg)	KehcC	0.016	Model fitted
Biliary elimination rate constant (L/h/kg)	KbileC	0.480	Model fitted
Fecal elimination rate constant (/h)	Kfeces	0.025	Model fitted

Note: Some parameters marked as “model fitted” were estimated by the PBPK model simulation using reported data (Xu et al., 2019a). Some parameters marked as “experimentally measured” were determined in the present study. If the parameter was obtained from the literature, the relevant references are listed. The tissue/plasma partition coefficients were calculated using the area under the concentration time curve (AUC) method based on the experimental pharmacokinetic (Xu et al., 2019b), and then further optimized with the tissue residue data (Xu et al., 2019a). These parameters were marked as “calculated/optimized”.

gill concentrations of DC after increasing the parameter value by 1%. The dose metrics of 24-h and 1008-h AUCs were selected to determine the impact of parameters on the early and terminal kinetic phases, respectively. Normalized sensitivity coefficient (NSC) was calculated using the equation reported previously and listed below (Lin et al., 2016a; Li et al., 2018):

$$NSC = \frac{\Delta r}{r} \times \frac{p}{\Delta p} \quad (1)$$

where r is the model output derived from the original parameter value, Δr is the change of model output resulting from 1% increase in the parameter value, p is the original parameter value, Δp is 1% of the original parameter value. The relative influence of each parameter on the response variables was categorized as being: low: $|NSC| < 0.2$; medium: $0.2 \leq |NSC| < 0.5$; and high: $0.5 \leq |NSC|$.

2.9. Monte Carlo (MC) analysis

MC analysis was employed to estimate the effects of parameter uncertainties and the intra-species variability of experimental animals on drug tissue residues and withdrawal intervals. Based on existing population PBPK studies (Zeng et al., 2017; Li et al., 2019), the relatively sensitive parameters that were identified by local SA were used to run MC analysis.

The physiological parameter of body weight was assumed as normal distribution, while chemical-specific parameters of PCs, Ka, PB, KehcC, Kbile, Kint, and KurineC were assumed as log-normal distribution. Coefficients of variance (CVs) for measured parameters were computed based on the collected data. For parameters without measured values, a default value of 20% was used for PCs, 30% for other chemical-specific parameters. Each Monto Carlo simulation was set as a batch run of 1000 iterations in Berkeley Madonna as we did in our recent study (Li et al., 2019). The lower bounds (i.e., 2.5th percentile) and upper bounds (i.e., 97.5th percentile) of model parameters were set in the model code of Berkeley Madonna. The values of parameters were randomly chosen from the defined distribution for each iteration during the MC simulation. WTs were determined as the times when doxycycline concentrations in the plasma and tissues fell below the MRLs for the 99% of the simulated population. In this study, local SA was performed at both 24 and 1008 h. Thus, two sets of sensitive parameters were identified. WTs in plasma and tissues were predicted by different MC simulations that were performed based on different sets of sensitive parameters identified at 24 h only, 1008 h only, and at 24 or 1008 h, respectively.

In the present study, WTs in plasma and tissues were also calculated using European Medicines Agency (EMA)'s WT 1.4 software and US Food and Drug Administration (FDA)'s “reschem” package with a tolerance limit of 99th percentile with a 95% confidence based on the residue data of DC after oral administrations at the dose of 20 mg/kg for 3 days (Xu et al., 2019a). Calculated WTs were compared to the PBPK-predicted WTs to evaluate the applicability of the PBPK model. The 99th percentile tolerance limit was used in the calculations in order for the calculated results to be comparable to the PBPK model-predicted results, which were based on 99% of the simulated population.

3. Results

3.1. Determination of cardiac output and organ weights

Cannulations of dorsal aorta and heart are technically highly difficult and require abundant experience. After repeated practice, the experiment was successfully completed, and the average cardiac output was calculated as 62.3 ± 15.3 mL/min/kg (n = 5) in grass carp based on the above-mentioned method.

The measured percentages of different organs accounted for the total body weight are listed in Table 2. The percentages for liver, kidney, muscle, skin, gill, and blood were 0.43%, 0.39%, 34.64%, 3.96%, 3.69%, and 7.41%, respectively. These measured parameter values were used in the PBPK model as shown in Table 1.

3.2. Pharmacokinetics of DC after intravenous injection

The concentrations of DC in plasma after intravenous treatment are listed in Table 3. These data could be best described with a two-compartment pharmacokinetic model. The relevant pharmacokinetic parameters, including distribution half-life ($t_{1/2\alpha}$), elimination half-life ($t_{1/2\beta}$), area under concentration–time curve ($AUC_{0-\infty}$), peak concentration (C_{max}), and volume of distribution at steady-state (Vss) were calculated as 0.24 h, 27.75 h, 975.78 h*mg/h, 147.44 mg/L, and 0.79 L/kg, respectively and are provided in Table S2 in the Supplementary Materials.

3.3. Model calibration

The model calibration results are shown in Fig. 2. The model-simulated kinetic profiles in liver, kidney, muscle + skin, and gill appropriately captured the observed concentrations. In the plasma, the model was able to simulate the observed concentrations for a few of the initial time points, but it greatly overestimated the terminal phase.

3.4. Model evaluation

The goodness of fit of the simulation results was evaluated by analysis of linear regression and MAPE. The values of R^2 calculated from linear regression between predicted and observed data were 0.93, 0.97, 0.79, 0.96 and 0.92 in plasma, liver, kidney, muscle + skin and gill, respectively. The value of R^2 for all predicted and observed data in both plasma and tissues was 0.93 (Fig. S1). The values of MAPE analyses were also calculated to be as 199.71%, 23.44%, 24.38%, 33.79% and 24.77% in plasma, liver, kidney, muscle + skin and gill, respectively. Overall, the model properly simulates the distribution of DC in the tissues, including liver, kidney, muscle + skin, and gill, but overestimates the plasma concentrations at the terminal phase.

3.5. Sensitivity analysis

Local SA was conducted to evaluate the influence on 24-h AUCs or 1008-h AUCs of plasma, liver, kidney, muscle + skin and gill in grass carp by increasing 1% of the parameter value for each of the 31 model parameters. Only the parameters with at least one absolute value of normalized sensitivity coefficient (NSC) equal to or more than 0.2 were considered as sensitive parameters and are listed in Table 4. The results showed that the sensitive parameters were somewhat different between 24 and 1008 h. At 24 h, the sensitive parameters were BW, PL, PK, PM, PG, Ka, KehcC, KbileC, and PB. At 1008 h, the sensitive parameters

Table 2
Experimentally measured percentages of blood and organs/tisssues out of the total body weight in grass carp (*Ctenopharyngodon idella*) (n = 10).

Tissues	Percentage (%)
Skin	3.96 ± 2.09
Muscle	34.64 ± 4.96
Heart	0.22 ± 0.064
Liver	0.43 ± 0.27
Spleen	0.068 ± 0.022
Gill	3.69 ± 1.13
Kidney	0.39 ± 0.26
Swim bladder	1.09 ± 0.36
Bile	1.13 ± 0.72
Gut	1.55 ± 0.60
Blood	7.41 ± 0.81
Remainder	45.42 ± 5.90

Note, the data are presented as mean ± SD.

Table 3
The concentrations of doxycycline in grass carp (*Ctenopharyngodon idella*) plasma after a single intravenous administration at 20 mg/kg (n = 6).

Time (h)	Concentration (mg/L)
0.08	152.75 ± 9.1
0.17	75.19 ± 6.93
0.50	56.61 ± 6.19
1.00	33.3 ± 7.73
2.00	31.96 ± 7.32
4.00	20.34 ± 4.69
6.00	18.07 ± 5.71
8.00	16.85 ± 5.35
16.00	12.85 ± 3.4
24.00	11.37 ± 3.24
48.00	7.32 ± 1.76
72.00	5.23 ± 1.54
96.00	2.79 ± 0.59
120.00	1.02 ± 0.58

Note, the data are presented as mean ± SD.

were BW, PL, PK, PM, PG, Ka, KehcC, KbileC, Kint, and KurineC. Kint and KurineC were not sensitive at 24 h, but became sensitive at the terminal kinetic phase of 1008 h. For other sensitive parameters, they were sensitive at both 24 and 1008 h with similar NSC values except for PB that was only sensitive at 24 h.

The SA results also showed that selected AUCs were insensitive to the changes of most physiological parameters except for BW with NSC values of 0.5 for each AUC except in liver and gill (0.49). The AUCs in liver, kidney, muscle + skin and gill were highly sensitive to PCs in corresponding tissues with NSC values more than 0.9. The AUCs of plasma, kidney, muscle + skin and gill were sensitive to Ka with same NSC values of 0.48 at 24 h or 0.41 at 1008 h and to KehcC with the same NSC values of 0.49 at 24 h or 0.46 at 1008 h. The AUCs of plasma, kidney, muscle + skin and gill were highly sensitive to KbileC with identical NSC values of −0.83, but to AUC in liver with a slightly different NCS value of −0.84 at 24 h. All selected AUCs were negatively sensitive to Kint at 1008 h with NSC value of −0.71 but were insensitive at 24 h. The selected AUCs of plasma, kidney, muscle + skin and gill were moderately sensitive to PB with NSC values from −0.22 to −0.20 at 24 h, but PB was not a sensitive parameter according to SA at 1008 h. The AUC of kidney was sensitive to KurineC with NSC value of −0.23 at 1008 h, but insensitive to KurineC at 24 h.

3.6. Monte Carlo analysis

The population analysis for DC's PBPK model in grass carp was executed using the MC method. The values and distributions of parameters used in the MC analysis for the PBPK model are listed in Table 5. Based on the regulatory guideline on MRLs of DC in EU, China and Japan, muscle + skin was considered as edible tissue (i.e., the target tissue) with stipulated MRL values of 100, 100, and 50 μg/kg, respectively. The estimated WTs using this population PBPK model were 40, 53, 42, 41 and 54 d for plasma, liver, kidney, muscle + skin and gill, respectively, based on the MRL value of 100 μg/kg from EU and China according to sensitive parameters identified at 24 h (Fig. 3, Fig. S2 and Table 6). According to sensitive parameters identified at 1008 h, WTs were estimated as 54, 73, 56, 54 and 74 d for plasma, liver, kidney, muscle + skin and gill, respectively (Fig. S4 and Table 6). In term of sensitive parameters identified at 24 or 1008 h, WTs were estimated as 54, 73, 56, 54 and 73 d for plasma, liver, kidney, muscle + skin and gill, respectively (Fig. S5 and Table 6). The estimated WT results using the traditional tolerance limit method with either the EMA's WT 1.4 software (Fig. S6) or US FDA's "reschem" package (Fig. S7) were 26, 61, 45, 43 and 49 d for plasma, liver, kidney, muscle + skin and gill, respectively. These results suggest that the PBPK model-predicted WTs based on sensitive parameters at 24 h are similar to the WTs estimated using the traditional tolerance limit method except in plasma. However, the PBPK model-predicted WTs based on sensitive parameters at 1008 h were much longer than the results estimated using traditional tolerance limit method. In the present study, the WTs after extra-label dose of 40 mg/kg (2 × label dose) for 3 daily doses were also predicted based on sensitive parameters at 24 h, and the results were 48 d in plasma, 62 d in liver, 49 d in kidney, 48 d in muscle + skin, and 62 d in gill, respectively (Fig. 3 and Fig. S3).

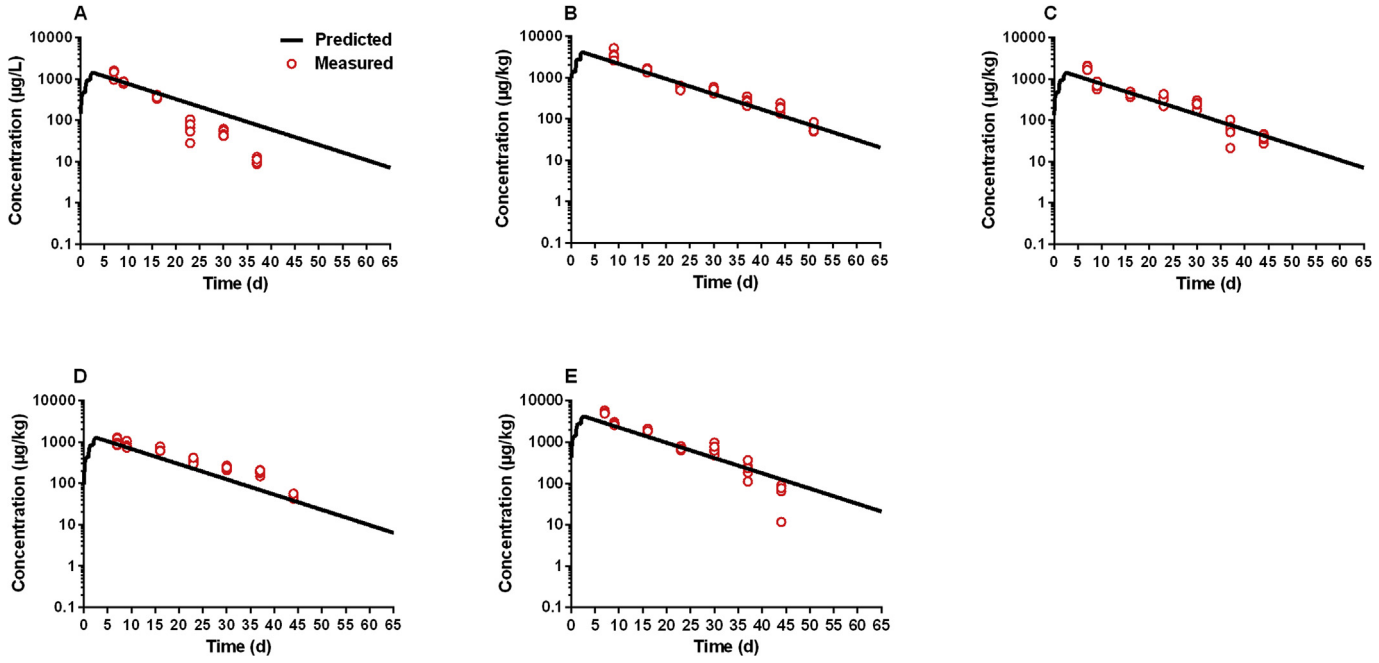

Fig. 2. PBPK model calibration results. Comparisons of model predictions (solid lines) and observed data (red circles) for doxycycline in plasma (A), liver (B), kidney (C), muscle (D) and gill (E) of grass carp (*Ctenopharyngodon idella*) following daily oral administrations at 20 mg/kg for 3 days. The experimental data are from Ning et al. (Xu et al., 2019a). (For interpretation of the references to colour in this figure legend, the reader is referred to the Web version of this article.)

Table 4
Sensitive parameters identified by the local sensitivity analysis.

Parameters	Normalized sensitivity coefficients (NSCs)									
	AUCCV		AUCCL		AUCCK		AUCCM		AUCCG	
	0–24 h	0–1008 h	0–24 h	0–1008 h	0–24 h	0–1008 h	0–24 h	0–1008 h	0–24 h	0–1008 h
BW	0.50	0.50	0.50	0.49	0.50	0.50	0.50	0.50	0.50	0.49
PL	–	–	0.99	1.00	–	–	–	–	–	–
PK	–	–	–	–	1.00	1.00	–	–	–	–
PM	–	–	–	–	–	–	0.91	1.00	–	–
PG	–	–	–	–	–	–	–	–	0.98	1.00
Ka	0.48	0.41	0.48	0.41	0.48	0.41	0.48	0.41	0.48	0.41
Kint	–	−0.71	–	−0.71	–	−0.71	–	−0.71	–	−0.71
KehcC	0.49	0.46	0.49	0.46	0.49	0.46	0.49	0.46	0.49	0.46
KbileC	−0.83	−0.83	−0.84	−0.83	−0.83	−0.83	−0.83	−0.83	−0.83	−0.83
PB	−0.20	–	–	–	−0.22	–	−0.22	–	−0.20	–
KurineC	–	–	–	–	–	−0.23	–	–	–	–

Note: represents a |NSC| less than 0.2. Only parameters with at least one absolute value of NSC equal to or more than 0.2 are presented in the table. AUCCV, AUCCL, AUCCK, AUCCM and AUCCG represent area under doxycycline concentration curves in the plasma, liver, kidney, muscle + skin, and gill, respectively.

Table 5
Values and distributions of parameters used in the Monte Carlo analysis for the PBPK model.

Abbreviation	Distribution	Mean	SD	CV	Lower bound	Upper bound
BW	Normal	0.450	5.320E-02*	0.118*	0.346	0.554
PL	Lognormal	2.821	5.642E-01	0.200	1.876	4.078
PK	Lognormal	1.064	2.128E-01	0.200	0.708	1.538
PM	Lognormal	0.901	1.802E-01	0.200	0.599	1.303
PG	Lognormal	2.981	5.926E-01	0.200	1.983	4.309
Ka	Lognormal	0.007	2.100E-03	0.300	0.004	0.012
Kint	Lognormal	0.003	9.300E-04	0.300	0.002	0.005
KehcC	Lognormal	0.016	4.800E-03	0.300	0.009	0.027
KbileC	Lognormal	0.480	1.440E-01	0.300	0.259	0.817
PB	Lognormal	0.900	2.700E-01	0.300	0.485	0.990
KurineC	Lognormal	0.019	5.580E-03	0.300	0.010	0.032

Note: A star sign (*) represents that the CV and SD were calculated based on the experimental data from this study. A default CV of 20% was used for partition coefficients, and a default CV of 30% was used for other parameters. The 2.5th and 97.5th percentile of each parameter were calculated as the lower and upper bounds, respectively.

Table 6
Withdrawal times in plasma, liver, kidney, muscle + skin and gill calculated using the PBPK model or the traditional tolerance method at the label dose of 20 mg/kg daily for three days.

Tissues	Withdrawal times (d)			
	Sensitive parameters identified at 24 and/or 1008 h			Traditional method (EMA)
	MC 0–24 h	MC 0–1008 h	MC all	
Plasma	40	54	54	26
Liver	53	73	73	61
Kidney	42	56	56	45
Muscle + skin	41	54	54	43
Gill	54	74	73	49

Note: MC 0–24 h represents Monte Carlo analysis results based on sensitive parameters identified at 24 h. MC 0–1008 h represents Monte Carlo analysis results based on sensitive parameters identified at 1008 h. MC all represents Monte Carlo analysis results based on sensitive parameters identified at either 24 or 1008 h. EMA, European Medicines Agency.

4. Discussion

In the present study, a PBPK model was established to predict plasma and tissue depletion in grass carp after exposure to DC for consecutive 3 days via oral administration. The model simulations well captured the depletion kinetics of DC in liver, kidney, muscle + skin and gill, and adequately predicted the WT in muscle + skin. This model will serve as a useful framework to develop PBPK models for other drugs in fish to aid fish-derived food safety assessment.

In this study, the important physiological parameter of cardiac

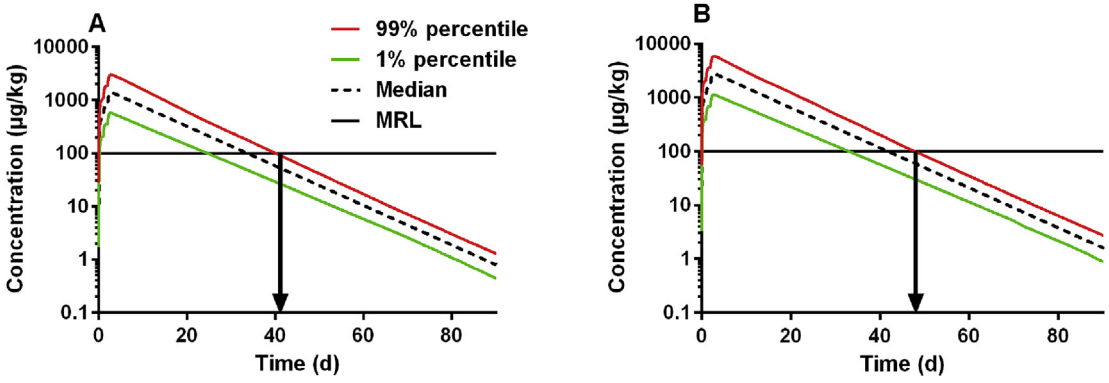

Fig. 3. Monte Carlo simulation result for doxycycline concentrations in grass carp (*Ctenopharyngodon idella*) according to the sensitivity analysis at 24 h. The median value (black dash lines), 99th percentile (red solid lines) and 1st percentile (green solid lines) of model predictions for doxycycline concentrations in muscle + skin of grass carp (*Ctenopharyngodon idella*) following daily oral administrations at label dose (20 mg/kg, A) or extra-label dose (40 mg/kg, B) for 3 days are shown in the figure. The horizontal black line represents the maximum residue limit of 100 μg/kg for doxycycline in fish in Europe and China. (For interpretation of the references to colour in this figure legend, the reader is referred to the Web version of this article.)

output for developing the PBPK model was determined experimentally for the first time in grass carp by indicator dilution method based on a published protocol (Barron et al., 1987). The indicator dilution approach has many strengths, including high accuracy, convenient operation, and low cost compared to Fick principle, perfused heart preparations, and flow-probe affixation methods, respectively (Linton et al., 2004). The approach of Fick principle to measure cardiac output in fish often produces unpredictable and inaccurate results due to overlooking the aerobic requirements of the gill and cutaneous oxygen uptake (Johansen and Pettersson, 1981). The method of perfused heart preparations is often used to elucidate mechanisms of physiological phenomena that are difficult to study in intact animals, but it is not well suited for descriptive studies (Graham and Farrell, 1989). As the development of bioelectronics, the flow-probe affixation method can be used to measure cardiac output in live and intact fish without complex surgery, but this method requires expensive instruments (Linton et al., 2005). By comparing the strengths and weaknesses of the available methods, the indicator dilution method was chosen to measure cardiac output of grass carp in the present study. Although this approach is relatively easy to operate than the perfused heart preparations method, it still has many technological difficulties, such as how to insert the corresponding cannula to dorsal aorta and heart. In order to find the accurate position, we carefully examined the physiological structures of dorsal aorta and heart by dissecting grass carp. Ultimately, the difficulties were overcome to warrant that the experiment procedure went smoothly. The measured results in this study were similar to that of rainbow trout (62.5 ± 4.3 mL/min/kg) with similar body weights to the present study at 18 °C (Barron et al., 1987), but the variability of cardiac output in grass carp was higher than rainbow trout. The exact reasons are unknown. It may be due to physiological differences between species, differences in the environmental temperatures, assay protocols, and measurement errors. The cardiac output is significantly influenced by temperature, and its value at 18 °C in rainbow trout is about two-fold of that at 12 °C (Barron et al., 1987). In the present study, we didn't determine cardiac outputs at different temperatures. However, this is a direction for future studies to extrapolate the model to other temperatures.

The present study did not consider potential sex differences in physiological parameters of fish. Similar to our study, many previous studies did not consider the potential discrepancy of physiological parameters between male and female fish (Stevens, 1968; Gingerich et al., 1987; Schultz et al., 1999; Yavuzcan-Yıldız and Kırkavgaç-Uzbilek, 2001). This was, partly, because it is difficult to distinguish the male from the female fish using visual inspection. Furthermore, data on sex-specific physiological parameters for grass carp were not found in the literature. Therefore, this model didn't consider the potential influence of sex on physiological parameters.

The current PBPK model structure was designed on the basis of grass carp physiology, physicochemical properties of DC, and requirements of food safety assessment. Since grass carp do not have stomach, the oral absorption module was described without the gastric emptying rate, which is different compared to the traditional method used for mammals (Lin et al., 2015; Zeng et al., 2017). In grass carp, the gut structure is less sophisticated than mammals, and is mainly separated into foregut, midgut and hindgut (Smith, 1980). Drug or food absorption mainly occurs in foregut and midgut and it probably occurs to some degree in the hindgut (Smith, 1980). Moreover, DC has been reported to encounter enterohepatic circulation in different animal species (Papich and Riviere, 2018), thus the enterohepatic circulation of DC was incorporated into the model to account for this mechanism. At the initial stage of developing this model, we tried different model structures to describe oral absorption, including (1) different absorption segments and enterohepatic circulation model, (2) enterohepatic circulation model not including different absorption segments, and (3) different absorption segments model not including enterohepatic circulation. The results showed that, if enterohepatic circulation was not included into the model, the model underestimated the observed concentrations of DC in tissues. If different absorption segments were not included in the model, the predicted kinetic profiles did not capture the observed profiles at the terminal phase in tissues. Therefore, the final model structure consisted of enterohepatic circulation and two different sites of absorption. Using this structure, the model can be used to predict the fraction of the drug eliminated by the bile (Abile) that was reabsorbed (Aehc). It was found that about 57.6% of the drug eliminated by the bile was reabsorbed from the intestine to the systemic circulation at 24 h after a single oral administration at 20 mg/kg.

In addition, Ka and Kint were estimated by model fitting as measured values were not available in grass carp. These values are less than those in swine and cattle for other drugs partly due to differences in physiology among different species or differences in physicochemical properties of different drugs (Zeng et al., 2017; Li et al., 2019). In the literature, comparative studies of Ka and Kint between fish and mammals are not available, but the comparison of Ka and Kint between fish with and without stomach has been reported. Specifically, it has been demonstrated that the digestion, absorption and excretion rates in tiger puffer (*Takifugu rubripes*) that have no stomach are significantly slower than in red sea bream (*Pagrus major*) that have a stomach by feeding test diets with an index compound of Cr_2O_3 (Takii et al., 1997). It is speculated that the lower Ka and Kint in grass carp is possibly because of the lack of stomach in grass carp and also because mammals possess higher efficiency of digestive and metabolic enzymes to accelerate the absorption speed in the gut (Saito et al., 2001).

Regarding model calibration, the residue data of DC in grass carp after repeated oral doses were used to calibrate the model because the main purpose of this model was to predict drug residue depletion and WTs in plasma and tissues in grass carp after multiple oral doses (i.e., the label use). The model was also used to simulate the observed data in grass carp following a single oral dose (Xu et al., 2019b), but the model underestimated the observed concentrations. It has been reported that pharmacokinetics between a single oral dose and multiple oral doses could be quite different (Samuelsen et al., 1997; Samuelsen, 2006). In the single oral dose study, the samples were collected only up to 7 days after drug administration and the samples were analyzed with a UPLC method (Xu et al., 2019b). On the other hand, in the multiple oral dose study, samples were collected up to 56 days after drug administrations and samples were analyzed with a more sensitive LC-MC/MS method (Xu et al., 2019a). In order to estimate the withdrawal interval after drug administration, it is required for the model to be able to simulate the terminal kinetic phase when the drug concentrations are lower than the MRL. Therefore, the repeated exposure study is more suitable to calibrate the model for drug residue predictions for a long period of time for the purpose of withdrawal interval estimation and food safety assessment. Future studies are needed to elucidate the underlying reasons in the pharmacokinetic differences of DC between single and multiple administrations. Additionally, fish are heterothermic animals. Many studies have reported that water temperature can remarkably affect drug pharmacokinetic in fish (Rigos et al., 2002, 2003; Rairat et al., 2019; Yang et al., 2020). Our recent study also showed that the pharmacokinetics of DC in grass carp was different between 18 and 24 °C (Xu et al., 2019b). Therefore, it is important to conduct tissue residue depletion studies at different temperatures and then extrapolate the present model to other temperatures in future studies.

During the PBPK model development, local SA was performed for 31 parameters at two time points of 24 h and 1008 h. The results showed that most of obtained sensitive parameters were the same at the two time points, except PB was sensitive only at 24 h, and Kint and KurineC were sensitive only at 1008 h. All physiological parameters were not highly sensitive to predicted AUCs except for body weight. The partition coefficients of liver, kidney, muscle + skin and gill were highly sensitive to AUCs of corresponding tissues but had low sensitivity for AUCs of other tissues. This result is expected because most of compounds' concentrations in tissues are directly related to partition

coefficients. The parameters related to absorption and enterohepatic circulation including Ka, KehcC and KbileC were highly influential on the predicted results because the PBPK model was established based on the treatment scenario of consecutive oral gavage, and DC undergoes enterohepatic circulation after oral administration (Papich and Riviere, 2018).

The MC sampling technique was used to analyze the population variation and estimate the WTs in plasma and tissues. In the previous studies, MC analysis was performed generally based on sensitive parameters identified at the early kinetic phase of 24 h (Huang et al., 2015a; Li et al., 2018; Zeng et al., 2019). However, in this study, since the model simulation lasted for more than 40 d, we performed SA to determine if the sensitive parameters were the same at early and terminal kinetic phases. The results showed that while most sensitive parameters were sensitive at both 24 and 1008 h, PB was sensitive only at 24 h, whereas Kint and KurineC were sensitive only at 1008 h. In order to determine the impact of these differential sensitive parameters on the predicted WTs, MC analysis was performed based on sensitive parameters at 24 h only, at 1008 h only, and at 24 or 1008 h. The results showed that the model-predicted values of WTs based on sensitive parameters at 24 h in kidney, muscle + skin, and gill based were close to the calculated WTs in corresponding tissues using WT 1.4 or "reschem" package. On the other hand, the model-predicted values of WTs based on sensitive parameters at 1008 h in plasma and tissues were much longer than the values calculated using the tolerance limit method. These results suggest that the concentration of DC at the early vs. the terminal kinetic phases is sensitive to different parameters, and this should be considered when performing population analysis to calculate WTs. In this regard, some of the previous PBPK models performed population analysis by considering the variability of all parameters (Li et al., 2017), which is more time-consuming, but this approach may capture the population variability more accurately.

In this model, the WTs were estimated using one MC population analysis of 1000 animals to calculate 99th percentile. In the literature, 100 or 1000 MC simulations of 1000 iterations each have been used to calculate 95% confidence intervals for the 99th percentile of the population for each tissue (Buur et al., 2006; Li et al., 2019). The calculated lower bound and upper bound using 95% confidence intervals are generally in a small range. These values after rounding up to the next whole day according to WT estimation criteria are consistent with the value of the WT using one MC simulation (Buur et al., 2006; Li et al., 2019). Therefore, the present method using one MC analysis with 1000 iterations for each tissue is sufficient to estimate WTs.

Overall, the present study suggests that PBPK models are a valuable tool in the estimation of WTs. Compared to traditional tolerance limit method, PBPK models are advantageous because they can be used to conduct extrapolation across doses, species, routes, etc. For example, as demonstrated in Fig. 3, the present model can be used to estimate WTs at extralabel doses, such as 2-fold, 5-fold, or even 10-fold of the label dose. This extrapolation would not be possible using tolerance limit method as the latter is data-based empirical method. However, there are limitations of PBPK models. Specifically, these models are complex and involve many parameters, and may require a great amount of experimental data, including in vivo data, to develop a model. Nevertheless, recent studies have made it possible to develop PBPK models solely based on in vitro and in silico approaches and can conduct read-across using PBPK models (i.e., extrapolation of PBPK models from one compound to another structurally similar compound) (Zhu et al., 2017; Ellison, 2018; Escher et al., 2019; Fabian et al., 2019). As more and more PBPK models are being developed in food animals (Lin et al., 2016a; Lautz et al., 2019), it is anticipated that PBPK models will become an important tool in the estimation of WTs of drugs in food animals.

Although the PBPK model adequately predicts DC's concentrations and WTs in tissues, it has some limitations. Firstly, this model does not consider potential influence of sex on physiological parameters and WTs. Secondly, the model could only simulate DC concentrations for a few initial time points in plasma but overestimates the plasma concentrations at the terminal phase. The exact reason of this overestimation is unknown, but it is possible that DC may be degraded by some substance in plasma that does not exist in tissues during the period of sample preservation (Von Wittenau et al., 1972; Axisa et al., 2000; Kim et al., 2013). Thirdly, this model fails to simulate the pharmacokinetics after a single oral dose. Fourthly, the PB value of DC was based on measured data in humans (Pal et al., 2018) as fish-specific data were not available. Fifthly, the Curve Fitting Module of Berkeley Madonna only provide the best value for each estimated parameter, without providing the uncertainty of each estimated value. Additionally, this model has not been comprehensively evaluated with independent datasets due to lack of other relevant data in the literature. In the future, fish-specific plasma protein binding and residue depletion studies in grass carp exposed to DC via oral gavage at different dose levels or different temperatures should be conducted to further improve the model.

In conclusion, the present study reports original data on measured cardiac output and organ weights in grass carp, as well as pharmacokinetic data of doxycycline in grass carp after single intravenous injection. Based on these new data and our previously published data, we develop a PBPK model that successfully simulates the kinetics of DC in tissues, including liver, kidney, muscle + skin and gill of grass carp following consecutive oral administrations for 3 days. The application of the population PBPK model coupled with MC simulations to estimate WTs in various tissues of grass carp demonstrates the feasibility of predicting WTs in fish using PBPK models. The present model provides a useful framework for extrapolating to different dosages, fish species or other tetracyclines to assess fish-derived food safety.

Author contribution

Ning Xu and Zhoumeng Lin conceived and designed study. Ning Xu, Miao Li and Wei-Chun Chou, and Zhoumeng Lin contributed to PBPK modeling and analysis. Ning Xu and Zhoumeng Lin contributed to data interpretation. Ning Xu drafted the manuscript. Zhoumeng Lin mentored and coordinated the project, and comprehensively revised the manuscript. All authors have read and approved the final manuscript.

Declaration of competing interest

The authors declare that they have no known competing financial interests or personal relationships that could have appeared to influence the work reported in this paper.

Acknowledgements

This study was supported by the Hubei Province Natural Science Foundation (2019CFB636) and the China Scholarship Council (Award #: 201803260013) to Dr. Ning Xu.

Transparency document

Transparency document related to this article can be found online at https://doi.org/10.1016/j.fct.2020.111127.

Appendix A. Supplementary data

Supplementary data to this article can be found online at https://doi.org/10.1016/j.fct.2020.111127.

References

Axisa, B., Naylor, A.R., Bell, P.R.F., Thompson, M.M., 2000. Simple and reliable method of doxycycline determination in human plasma and biological tissues. J. Chromatogr.

B Biomed. Appl. 744, 359–365. https://doi.org/10.1016/S0378-4347(00)00261-9.
Barron, M.G., Tarr, B.D., Hayton, W.L., 1987. Temperature-dependence of cardiac output and regional blood flow in rainbow trout, *Salmo gairdneri Richardson*. J. Fish Biol. 31, 735–744. https://doi.org/10.1111/j.1095-8649.1987.tb05276.x.
Baynes, R.E., Dedonder, K., Kissell, L., Mzyk, D., Marmulak, T., Smith, G., Tell, L., Gehring, R., Davis, J., Riviere, J.E., 2016. Health concerns and management of select veterinary drug residues. Food Chem. Toxicol. 88, 112–122. https://doi.org/10.1016/j.fct.2015.12.020.
Buur, J., Baynes, R., Smith, G., Riviere, J., 2006. Use of probabilistic modeling within a physiologically based pharmacokinetic model to predict sulfamethazine residue withdrawal times in edible tissues in swine. Antimicrob. Agents Chemother. 50, 2344–2351. https://doi.org/10.1128/Aac.01355-05.
Ellison, C.A., 2018. Structural and functional pharmacokinetic analogs for physiologically based pharmacokinetic (PBPK) model evaluation. Regul. Toxicol. Pharmacol. 99, 61–77. https://doi.org/10.1016/j.yrtph.2018.09.008.
EMA, 2009. Guideline on studies to evaluate the metabolism and residue kinetics of veterinary drugs in food-producing animals: marker residue depletion studies to establish product withdrawal periods. https://www.ema.europa.eu/en/documents/scientific-guideline/vich-topic-gl48-step-4-guideline-studies-evaluate-metabolism-residue-kinetics-veterinary-drugs-food_en.pdf.
Escher, S.E., Kamp, H., Bennekou, S.H., Bitsch, A., Fisher, C., Graepel, R., Hengstler, J.G., Herzler, M., Knight, D., Leist, M., Norinder, U., Ouédraogo, G., Pastor, M., Stuard, S., White, A., Zdrazil, B., van de Water, B., Kroese, D., 2019. Towards grouping concepts based on new approach methodologies in chemical hazard assessment: the read-across approach of the EU-ToxRisk project. Arch. Toxicol. 93, 3643–3667. https://doi.org/10.1007/s00204-019-02591-7.
EU, 2015. Commission regulation (EU) 2015/151 of 30 january 2015 amending the annex to regulation (EU) No 37/2010 as regards the substance 'doxycycline'. Off. J. Eur. Union L 26/13. https://eur-lex.europa.eu/legal-content/EN/TXT/PDF/?uri=CELEX:32015R0151&from=EN.
Fabian, E., Gomes, C., Birk, B., Williford, T., Hernandez, T.R., Haase, C., Zbranek, R., van Ravenzwaay, B., Landsiedel, R., 2019. In vitro-to-in vivo extrapolation (IVIVE) by PBTK modeling for animal-free risk assessment approaches of potential endocrine-disrupting compounds. Arch. Toxicol. 93, 401–416. https://doi.org/10.1007/s00204-018-2372-z.
FAO, 2018. The State of World Fisheries and Aquaculture - Meeting the Sustainable Development Goals. F.a.A.O.o.t.U. Nations, Rome : FAO. https://www.fao.org/3/a-i3720e.pdf.
Gingerich, W.H., Pityer, R.A., Rach, J.J., 1987. Estimates of plasma, packed cell and total blood volume in tissues of the rainbow trout (*Salmo gairdneri*). Comp. Biochem. Physiol. A Physiol. 87, 251–256. https://doi.org/10.1016/0300-9629(87)90119-8.
Graham, M., Farrell, A., 1989. The effect of temperature acclimation and adrenaline on the performance of a perfused trout heart. Physiol. Zool. 62, 38–61.
Grech, A., Brochot, C., Dorne, J.L., Quignot, N., Bois, F.Y., Beaudouin, R., 2017. Toxicokinetic models and related tools in environmental risk assessment of chemicals. Sci. Total Environ. 578, 1–15. https://doi.org/10.1016/j.scitotenv.2016.10.146.
Grech, A., Tebby, C., Brochot, C., Bois, F.Y., Bado-Nilles, A., Dorne, J.L., Quignot, N., Beaudouin, R., 2019. Generic physiologically-based toxicokinetic modelling for fish: integration of environmental factors and species variability. Sci. Total Environ. 651, 516–531. https://doi.org/10.1016/j.scitotenv.2018.09.163.
Hu, K., Chen, K., Zhou, X.Q., 2019. A comparative study: effects of the coated slow-release multi-trace elements and trace elements on growth performance, digestion and absorption capacities and growth development in the intestine of young grass carp (*Ctenopharyngodon idella*). J. Sichuan Agric. Univ. 37, 557–565. https://doi.org/10.16036/j.issn.1000-2650.2019.04.018.
Huang, L., Lin, Z., Zhou, X., Zhu, M., Gehring, R., Riviere, J.E., Yuan, Z., 2015a. Estimation of residue depletion of cyadox and its marker residue in edible tissues of pigs using physiologically based pharmacokinetic modelling. Food Addit. Contam. A 32, 2002–2017. https://doi.org/10.1080/19440049.2015.1100330.
Huang, L., Xu, N., Harnud, S., Pan, Y., Chen, D., Tao, Y., Liu, Z., Yuan, Z., 2015b. Metabolic disposition and elimination of cyadox in pigs, chickens, carp, and rats. J. Agric. Food Chem. 63, 5557–5569. https://doi.org/10.1021/acs.jafc.5b01745.
JFCRF, 2006. The Japan food chemical Research foundation (JFCRF) enforcement on 29 may 2006 of the Japanese positive list system for agricultural chemical residues in foods food safety and comsumer affairs bureau. NO. 12-33. https://db.ffcr.or.jp/front/pesticide_detail?id=43400.
Johansen, K., Pettersson, K., 1981. Gill O2 consumption in a teleost fish, Gadus morhua. Respir. Physiol. 44, 277–284. https://doi.org/10.1016/0034-5687(81)90023-2.
Kim, K.-S., Yang, C.-S., Mok, Y.S., 2013. Degradation of veterinary antibiotics by dielectric barrier discharge plasma. Chem. Eng. J. 219, 19–27. https://doi.org/10.1016/j.cej.2012.12.079.
Lautz, L.S., Oldenkamp, R., Dorne, J.L., Ragas, A.M.J., 2019. Physiologically based kinetic models for farm animals: critical review of published models and future perspectives for their use in chemical risk assessment. Toxicol. In Vitro 60, 61–70. https://doi.org/10.1016/j.tiv.2019.05.002.
Law, F.C.P., 1999. A physiologically based pharmacokinetic model for predicting the withdrawal period of oxytetracycline in cultured chinook salmon (*Oncorhynchus tshawytscha*). In: Smith, D.J., Gingerich, W.H., Beconi-Barker, M.G. (Eds.), Xenobiotics in Fish. Kluwer Academic/Plenum Publishers, New York.
Law, F.C.P., Abedini, S., Kennedy, C.J., 1991. A biologically based toxicokinetic model for pyrene in rainbow trout. Toxicol. Appl. Pharmacol. 110, 390–402. https://doi.org/10.1016/0041-008X(91)90041-C.
Leavens, T.L., Tell, L.A., Kissell, L.W., Smith, G.W., Smith, D.J., Wagner, S.A., Shelver, W.L., Wu, H., Baynes, R.E., Riviere, J.E., 2014. Development of a physiologically based pharmacokinetic model for flunixin in cattle (*Bos taurus*). Food Addit. Contam. A 31, 1506–1521. https://doi.org/10.1080/19440049.2014.938363.
Li, M., Cheng, Y.-H., Chittenden, J.T., Baynes, R.E., Tell, L.A., Davis, J.L., Vickroy, T.W., Riviere, J.E., Lin, Z., 2019. Integration of Food Animal Residue Avoidance Databank (FARAD) empirical methods for drug withdrawal interval determination with a mechanistic population-based interactive physiologically based pharmacokinetic (iPBPK) modeling platform: example for flunixin meglumine administration. Arch. Toxicol. https://doi.org/10.1007/s00204-019-02464-z.
Li, M., Gehring, R., Riviere, J.E., Lin, Z., 2017. Development and application of a population physiologically based pharmacokinetic model for penicillin G in swine and cattle for food safety assessment. Food Chem. Toxicol. 107, 74–87. https://doi.org/10.1016/j.fct.2017.06.023.
Li, M., Gehring, R., Riviere, J.E., Lin, Z.M., 2018. Probabilistic physiologically based pharmacokinetic model for penicillin G in milk from dairy cows following intramammary or intramuscular administrations. Toxicol. Sci. 164, 85–100. https://doi.org/10.1093/toxsci/kfy067.
Lin, Z., Gehring, R., Mochel, J.P., Lavé, T., Riviere, J.E., 2016a. Mathematical modeling and simulation in animal health – Part II: principles, methods, applications, and value of physiologically based pharmacokinetic modeling in veterinary medicine and food safety assessment. J. Vet. Pharmacol. Ther. 39, 421–438. https://doi.org/10.1111/jvp.12311.
Lin, Z., Jaberi-Douraki, M., He, C., Jin, S., Yang, R.S.H., Fisher, J.W., Riviere, J.E., 2017. Performance assessment and translation of physiologically based pharmacokinetic models from acslX to Berkeley Madonna, MATLAB, and R Language: oxytetracycline and gold nanoparticles as case examples. Toxicol. Sci. 158, 23–35. https://doi.org/10.1093/toxsci/kfx070.
Lin, Z., Li, M., Gehring, R., Riviere, J.E., 2015. Development and application of a multiroute physiologically based pharmacokinetic model for oxytetracycline in dogs and humans. J. Pharm. Sci. 104, 233–243. https://doi.org/10.1002/jps.24244.
Lin, Z., Monteiro-Riviere, N.A., Riviere, J.E., 2016b. A physiologically based pharmacokinetic model for polyethylene glycol-coated gold nanoparticles of different sizes in adult mice. Nanotoxicology 10, 162–172. https://doi.org/10.3109/17435390.2015.1027314.
Linton, E., Scruton, D., McKinley, R.S., 2004. Cardiac output in fish: measurement techniques and applications. Fish. Oceans.
Linton, E., Scuton, D., McKinley, R., 2005. Physiological effects of thermomechanical newsprint mill effluent on Atlantic salmon (*Salmo salar L.*). Ecotoxicol. Environ. Saf. 62, 317–330. https://doi.org/10.1016/j.ecoenv.2004.09.002.
Liu, R., Lian, Z., Hu, X., Lü, A., Sun, J., Chen, C., Liu, X., Song, Y., Yiksung, Y., 2019. First report of *Vibrio vulnificus* infection in grass carp *Ctenopharyngodon idellus* in China. Aquaculture 499, 283–289. https://doi.org/10.1016/j.aquaculture.2018.09.051.
Liu, X., Steele, J.C., Meng, X.Z., 2017. Usage, residue, and human health risk of antibiotics in Chinese aquaculture: a review. Environ. Pollut. 223, 161–169. https://doi.org/10.1016/j.envpol.2017.01.003.
Lulijwa, R., Rupia, E.J., Alfaro, A.C., 2019. Antibiotic use in aquaculture, policies and regulation, health and environmental risks: a review of the top 15 major producers. Rev. Aquac. https://doi.org/10.1111/raq.12344.
MAA, 2017. National Food Safety Standard(approval Draft)- Maximum Residue Limits for Veterinary Drugs in Animal Derived Food.
Macey, R., Oster, G., Zahnley, T., 2009. Berkeley Madonna User's Guide. University of California, Berkeley, CA 94720. https://www.berkeleymadonna.com/system/storage/download/BM-Users-Guide-8.0.2.pdf.
Pal, A., Matzneller, P., Gautam, A., Österreicher, Z., Wulkersdorfer, B., Reiter, B., Stimpfl, T., Zeitlinger, M., 2018. Target site pharmacokinetics of doxycycline for rosacea in healthy volunteers is independent of the food effect. Br. J. Clin. Pharmacol. 84, 2625. https://doi.org/10.1111/bcp.13721.
Papich, M.G., Riviere, J.E., 2018. Tetracycline antibiotics. In: Riviere, J.E., Pahich, M.G. (Eds.), Veterinary Pharmacology and Therapeutics, tenth ed. John Wiley & Sons Inc, Hoboken, NJ, pp. 858–876.
Rairat, T., Hsieh, C.Y., Thongpiam, W., Sung, C.H., Chou, C.C., 2019. Temperature-dependent pharmacokinetics of florfenicol in Nile tilapia (*Oreochromis niloticus*) following single oral and intravenous administration. Aquaculture. https://doi.org/10.1016/j.aquaculture.2018.12.081.
Rigos, G., Alexis, M., Andriopoulou, A., Nengas, I., 2002. Temperature-dependent pharmacokinetics and tissue distribution of oxolinic acid in sea bass, *Dicentrarchus labrax L.*, after a single intravascular injection. Aquacult. Res. 33, 1175–1181. https://doi.org/10.1046/j.1365-2109.2002.00783.x.
Rigos, G., Nengas, I., Alexis, M., Tyrpenou, A.E., Troisi, G.M., 2003. Tissue distribution and residue depletion of oxolinic acid in gilthead sea bream (*Sparus aurata*) and sharpsnout sea bream (*Diplodus puntazzo*) following multiple in-feed dosing. Aquaculture 224, 245–256. https://doi.org/10.1016/s0044-8486(03)00213-8.
Saito, M., Kitamura, H., Sugiyama, K., 2001. Liver gangliosides of various animals ranging from fish to mammalian species. Comp. Biochem. Physiol. B Biochem. Mol. Biol. 129, 747–758. https://doi.org/10.1016/S1096-4959(01)00379-7.
Samuelsen, O.B., 2006. Absorption, tissue distribution, metabolism and excretion of ormetoprim and sulphadimethoxine in cod (*Gadus morhua*) after oral administration of Romet(30). J. Appl. Ichthyol. 22, 68–71. https://doi.org/10.1111/j.1439-0426.2006.00703.x.
Samuelsen, O.B., Pursell, L., Smith, P., Ervik, A., 1997. Multiple-dose pharmacokinetic study of Romet30 in Atlantic salmon (*Salmo salar*) and in vitro antibacterial activity against *Aeromonas salmonicida*. Aquaculture 152, 13–24. https://doi.org/10.1016/S0044-8486(96)01508-6.
Schultz, I.R., Barron, M.G., Newman, M.C., Vick, A.M., 1999. Blood flow distribution and tissue allometry in channel catfish. J. Fish Biol. 54, 1275–1286. https://doi.org/10.1111/j.1095-8649.1999.tb02054.x.
Shireman, J.V., Colle, D.E., Rottman, R.W., 1976. Incidence and treatment of columnaris disease in grass carp brood stock. Prog. Fish-Cult. 38, 116–117. https://doi.org/10.1577/1548-8659(1976)38[116:IATOCD]2.0.CO;2.

Smith, L., 1980. Digestion in teleost fishes. Lectures presented at the FAO/UNDP Training course in fish feeding technology. ACDP/REP/80/11 3–17.

Stevens, E.D., 1968. The effect of exercise on the distribution of blood to various organs in rainbow trout. Comp. Biochem. Physiol. 25, 615–625. https://doi.org/10.1016/0010-406X(68)90372-1.

Takii, K., Konishi, K., Ukawa, M., Nakamura, M., Kumai, H., 1997. Comparison of digestive and absorptive functions between tiger puffer and red sea bream. Fish. Sci. 63, 349–354. https://doi.org/10.2331/fishsci.63.349.

Viola, S., Mokady, S., Arieli, Y., 1983. Effects of soybean processing methods on the growth of carp (*Cyprinus carpio*). Aquaculture 32, 27–38. https://doi.org/10.1016/0044-8486(83)90267-3.

Von Wittenau, M.S., Twomey, T., Swindell, A.C., 1972. The disposition of doxycycline by the rat. Chemotherapy 17, 26–39.

WHO, 2010. Characterization and Application of Physiologically Based Pharmacokinetic Models in Risk Assessment. I.P.o.C.S.W.I. World Health Organization, Geneva, Switzerland. https://apps.who.int/iris/bitstream/handle/10665/44495/9789241500906_eng.pdf.

Xu, N., Li, M., Fu, Y., Zhang, X., Ai, X., Lin, Z., 2019a. Tissue residue depletion kinetics and withdrawal time estimation of doxycycline in grass carp, *Ctenopharyngodon idella*, following multiple oral administrations. Food Chem. Toxicol. 131, 110592. https://doi.org/10.1016/j.fct.2019.110592.

Xu, N., Li, M., Fu, Y., Zhang, X., Dong, J., Liu, Y., Zhou, S., Ai, X., Lin, Z., 2019b. Effect of temperature on plasma and tissue kinetics of doxycycline in grass carp (*Ctenopharyngodon idella*) after oral administration. Aquaculture 511, 734204. https://doi.org/10.1016/j.aquaculture.2019.734204.

Yang, F., Lin, Z., Riviere, J.E., Baynes, R.E., 2019. Development and application of a population physiologically based pharmacokinetic model for florfenicol and its metabolite florfenicol amine in cattle. Food Chem. Toxicol. 126, 285–294. https://doi.org/10.1016/j.fct.2019.02.029.

Yang, F., Sun, N., Sun, Y.X., Shan, Q., Zhao, H.Y., Zeng, D.P., Zeng, Z.L., 2013. A physiologically based pharmacokinetics model for florfenicol in crucian carp and oral-to-intramuscular extrapolation. J. Vet. Pharmacol. Ther. 36, 192–200. https://doi.org/10.1111/j.1365-2885.2012.01419.x.

Yang, F., Yang, F., Wang, G., Kong, T., Wang, H., Zhang, C., 2020. Effects of water temperature on tissue depletion of florfenicol and its metabolite florfenicol amine in crucian carp (Carassius auratus gibelio) following multiple oral doses. Aquaculture 515, 734542. https://doi.org/10.1016/j.aquaculture.2019.734542.

Yang, X., Zhou, Y.F., Yu, Y., Zhao, D.H., Shi, W., Fang, B.H., Liu, Y.H., 2015. A physiologically based pharmacokinetic model for quinoxaline-2-carboxylic acid in rats, extrapolation to pigs. J. Vet. Pharmacol. Ther. 38, 55–64. https://doi.org/10.1111/jvp.12143.

Yavuzcan-Yıldız, H., Kırkavgaç-Uzbilek, M., 2001. The evaluation of secondary stress response of grass carp (*Ctenopharyngodon idella*, Val. 1844) after exposing to the saline water. Fish Physiol. Biochem. 25, 287–290. https://doi.org/10.1023/a:1023279604975.

Zeng, D., Lin, Z., Fang, B., Li, M., Gehring, R., Riviere, J.E., Zeng, Z., 2017. Pharmacokinetics of mequindox and its marker residue 1,4-bisdesoxymequindox in swine following multiple oral gavage and intramuscular administration: an experimental study coupled with population physiologically based pharmacokinetic modeling. J. Agric. Food Chem. 65, 5768–5777. https://doi.org/10.1021/acs.jafc.7b01740.

Zeng, D., Lin, Z., Zeng, Z., Fang, B., Li, M., Cheng, Y.-H., Sun, Y., 2019. Assessing global human exposure to T-2 toxin via poultry meat consumption using a lifetime physiologically based pharmacokinetic model. J. Agric. Food Chem. 67, 1563–1571. https://doi.org/10.1021/acs.jafc.8b07133.

Zhu, X., Huang, L., Xu, Y., Xie, S., Pan, Y., Chen, D., Liu, Z., Yuan, Z., 2017. Physiologically based pharmacokinetic model for quinocetone in pigs and extrapolation to mequindox. Food Addit. Contam. A 34, 192–210. https://doi.org/10.1080/19440049.2016.1258121.